

THREE-DIMENSIONAL TURBULENT VELOCITY FLUCTUATION MEASUREMENTS USING MAGNETIC RESONANCE IMAGING

Christopher J. Elkins

Mechanical Engineering Department
Stanford University
Stanford, CA 94305, USA
celkins@stanford.edu

Marcus Alley

Department of Radiology
Stanford University
Stanford, CA 94305, USA
mtalley@stanford.edu

Lars Sætran

Dept. of Energy and Process Engineering
Norwegian Univ. of Science and Technology
Trondheim, Norway
lars.satran@ntnu.no

John K. Eaton

Mechanical Engineering Department
Stanford University
Stanford, CA 94305, USA
eatonj@stanford.edu

ABSTRACT

Experimental measurements made using Magnetic Resonance Velocimetry (MRV), a technique based on Magnetic Resonance Imaging (MRI) principles, are presented for the 3D velocity field in the turbulent flow downstream of a backward facing step in a square channel with a Reynolds number of 48,000 based on the step height and the freestream velocity at the step edge. Results include the three-component mean velocity field measured using phase-contrast MRI methods and turbulent Reynolds stresses measured using a method based on diffusion imaging principles. MRV results are compared to particle image velocimetry (PIV) measurements made in the centerplane of the flow at several locations downstream of the step. The MRV and PIV mean velocity measurements show excellent agreement in all regions of the flow. The MRV measurements for the Reynolds normal stresses are in agreement with the PIV to within +/-20%.

INTRODUCTION

Most technological and natural flows are three-dimensional, turbulent, and highly complex making them difficult to predict accurately with computations. Even the most advanced conventional laser-based measurement techniques are either too time-consuming, too expensive, or simply incapable of measuring the entire flow fields for many of these real flows. Magnetic resonance velocimetry (MRV) presents an experimental alternative for use in these flows. MRV is a non-invasive technique for measuring the full 3D three-component mean velocity field and the turbulent velocity fluctuations for complex flows in and around opaque objects (Elkins et al. 2003; Elkins et al. 2004).

Past developments in magnetic resonance techniques for measuring turbulent fluctuations have focused primarily on 2D cross sections of turbulent pipe flow (Gao and Gore 1991, Li et al. 1994, Gatenby and Gore 1996) and stenotic (partially obstructed) pipes (Gatenby and Gore 1994; Dyverfeldt et al. 2006) because of the relevance to physiological flow through blood vessels. Many studies (De Gennes 1969; Kuethe 1989; Gao and Gore 1991; Gatenby

and Gore 1994; Kuethe and Gao 1995; and Dyverfeldt et al. 2006) use methods based on diffusion principles in which turbulence causes a loss of the net magnetization signal. The amount of signal loss is measured and related to the turbulent velocity statistics.

In this paper, we present an extension of the method of Gao and Gore (1991) to provide full-field 3D measurements of the turbulent Reynolds stresses. Although our basic method is similar to previous work, it relies on an experimental calibration method rather than theory and analysis to produce quantitative turbulence measurements.

The objective of this experiment was to test MRV techniques for measuring mean velocities and velocity fluctuations in a well-documented canonical three-dimensional turbulent flow: the flow downstream of a backward facing step in a square channel. The backward facing step flow affords quantitative characterization of the MRV results in the presence of a growing shear layer with variable mean shear rates and a large range of turbulent stress levels.

METHODS AND MATERIALS

MR System and Sequence

Hydrogen nuclei in a strong magnetic field, \vec{B} , align their spins with the direction of the field, typically defined as the z-direction. Radio frequency pulses at the resonant frequency, $\omega_0 = \gamma |\vec{B}| / 2\pi$, cause these nuclei to orient their spins perpendicular to the main magnetic field direction thereby obtaining "transverse magnetization." The traditional Bloch-Torrey equation describes the time evolution of the nuclei magnetization vector, \vec{M} , which is a function of the main magnetic field, magnetic field gradients, bulk nuclei motion, and molecular diffusion. MRI images are constructed from measurements of the magnitudes of the components of this vector. Kuethe (1989) presents a modified Bloch-Torrey equation for the complex "transverse magnetization" density function $m(\vec{x}, t)$ in a moving turbulent fluid,

$$\frac{\partial m}{\partial t} = -i\omega_0 m - i\gamma \vec{x} \cdot \vec{G} m - \frac{m}{T_2^*} - \nabla(\vec{V}_0 m) + \nabla((D_m + D_t)\nabla m)$$

where $i = \sqrt{-1}$, ω_0 is the angular velocity in the primary magnetic field, γ is the nuclear gyromagnetic ratio, \vec{x} is the position vector, \vec{G} is a magnetic field gradient, T_2^* is the time constant for the exponential decay of the transverse magnetization, \vec{V}_0 is the mean velocity of the fluid, D_m is the molecular diffusion coefficient, and D_t is the turbulent diffusion coefficient. In order to simplify the analysis, the turbulent diffusion coefficient is assumed to be constant and much larger than D_m . By applying a bipolar magnetic field gradient in addition to imaging gradients, an image of a flow can be created in which the signal magnitude S in each voxel is a measure of the average value of $m(\vec{x}, t)$. S is related to the quantities above by the relation

$$S = S_0 e^{-g(\tau, G)\gamma^2 D_t}$$

where τ is the duration of the bipolar gradient, G is the amplitude of the bipolar gradient, $g(\tau, G)$ is a function that describes the bipolar gradient waveform, and S_0 is the signal magnitude measured with $G = 0$. The signal loss can be increased by increasing the bipolar gradient amplitude, the duration of the bipolar gradient, and the turbulent diffusion. The gradient amplitude and timing are often combined into the first moment of the gradient defined as $M_1 = \int_0^\tau t' G(t') dt'$.

Following Gao and Gore (1991), we use the relation from Batchelor (1949) who modeled the diffusion coefficient for isotropic turbulence as

$$D_t(t) = \langle u'^2 \rangle \int_{t_0}^t R_L(t') dt'$$

where $\langle u'^2 \rangle$ is the variance of the fluctuating velocity and $R_L(t') = \langle u'(t)u'(t+t') \rangle / u'^2$ is the Lagrangian velocity autocorrelation coefficient. If the time $(t - t_0) = \tau$ is sufficiently short so that $R_L \approx 1$, we get $D_t = \sigma_u^2 \tau$,

where $\sigma_u \equiv \sqrt{\langle u'^2 \rangle}$. Substituting for D_t and defining

$$f(\tau, G) = \tau \gamma^2 g(\tau, G), \text{ gives the result}$$

$$S = S_0 e^{-f(\tau, G)\sigma_u^2}$$

and the variance of the fluctuating velocity can be found from the equation $\sigma_u^2 = \ln(S_0 / S) / f(\tau, G)$ once $f(\tau, G)$ is known. Several authors present different results for this function depending on their assumptions about the characteristics of the turbulence and the timing of the gradient sequence (De Gennes 1969; Gao and Gore 1991; Gatenby and Gore 1994; Kuethe and Gao 1995; and Dyverfeldt et al. 2006). For instance, Dyverfeldt, et al. derive the formula $\sigma_u^2 = 2 \ln(S_0 / S) / k_v^2$ where $k_v = 2\pi M_1$.

In the current experiment, $f(\tau, G)$ is simplified to $G^2 h(\tau)$ by varying the bipolar gradient amplitude while keeping the timing constant. A method similar to that of Gao and Gore (1991) is applied in which a least squares fit of $\ln(S_0 / S)$ vs. G^2 is used to determine $\sigma_u^2 h(\tau)$, and the function $h(\tau)$ is calibrated using one component of turbulent velocity measured at one point in the flow domain. Using this one point calibration, the turbulent fluctuations are measured throughout the entire flow domain with the gradient sequence described below. Since the bipolar gradients can be applied along different directions without changing the sequence timing and $h(\tau)$, fluctuating velocity components in other directions are measured using the same value for $h(\tau)$.

This technique for measuring fluctuating velocities relies on the dephasing of the spin signals coming from the turbulent regions of the flow. The turbulence causes the signal loss in a measurement volume through both intravoxel dephasing and ghosting artifacts. The ghosting artifacts occur because the randomness of the turbulence produces a change in the velocity distribution within a voxel from measurement to measurement. Because these signal changes are not consistent throughout the scan, the modulation of the k-space data will disperse signal from one pixel to other image pixels. The extent of the effect can be measured by looking at the signal magnitudes in the regions outside of the flow channel in the MR images. Ghosting artifacts and other signal to noise issues contribute largely to the uncertainty of the turbulent velocity measurements.

This uncertainty, $d\sigma_u$, can be estimated by using the equation,

$$d\sigma_u = \frac{\sqrt{\left(\frac{dS_0}{S_0}\right)^2 + \left(\frac{dS}{S}\right)^2}}{2\sigma_u G^2 h(\tau)}$$

where dS_0 is an estimate of the uncertainty in S_0 and measured as the signal magnitude outside of the flow channel in the $G = 0$ image and dS is an estimate of the uncertainty in S and measured as the signal magnitude outside of the flow channel in a $G > 0$ image. The equation shows that the uncertainty increases as the turbulent velocity decreases. In many cases large relative uncertainties in small values of the turbulence intensity are acceptable. However, this indicates that the present technique is not appropriate for turbulence measurements in low-turbulence flows. The equation also predicts that the uncertainty increases when the turbulence levels rise due to the increased ghosting signal and the decreased overall signal. In choosing the optimal bipolar gradient amplitudes, it is important to minimize this effect while creating enough signal reduction to accurately measure the velocity fluctuations. Typically, a magnitude reduction of ~50% works well.

The turbulence measurements were made using a 3D, RF-spoiled, gradient echo MR sequence. The turbulence encoding was done with a bipolar pair of gradients that could be played out along any combination of axes.

Experiments were performed on a 1.5-T MR system (GE Signa CV/I, $G_{\max} = 40\text{mT/m}$, rise time = $268\mu\text{s}$), with a single channel, extremity receive coil. Data were collected with a coronal slab chosen so that the field-of-view (FOV) was 280 mm in the streamwise and cross stream directions, and 60 1 mm thick slices were prescribed to cover the extent of the flow model in the spanwise direction. The in-plane matrix resolution was chosen to be 256 by 256 pixels, and a 0.3 fractional FOV in the phase encoding (cross stream) direction was used since the geometry is narrow in this direction. Other scan parameters included a flip angle of 25 degrees and a receiver bandwidth of $\pm 125\text{kHz}$. The resulting sequence repetition time (TR) and echo time (TE) were 5.0 and 3.7ms, respectively. A complete dataset was acquired in 27 seconds.

A large number of signal acquisitions (NSA) was prescribed to increase the signal-to-noise ratio (SNR) of the data, and for each acquisition, a complete set of 3D data in k-space was acquired before the next was begun. The temporal spacing between acquisitions of a given k-space position was the scan time of a single dataset. An NSA of 25 was prescribed, and the total scan time was 11.5 minutes.

In addition to measuring the turbulent fluctuations, the full three-dimensional velocity field was measured using the phase-contrast MRV method described in Elkins et al. (2003) modified to scan without the cine MRI functionality. These measurements were performed on the 1.5 Tesla system with a single channel, head-only receive coil. The measurement domain contained the entire flow channel starting upstream of the converging flow before the step and extending 8 step heights downstream. This 3D volume was scanned with a slab thickness of 64 mm and a FOV of 300 mm. The imaging matrix was $64 \times 256 \times 256$ which gave a voxel resolution of $1.0 \text{ mm} \times 1.2 \text{ mm} \times 1.2 \text{ mm}$. A 0.5 fractional FOV was used in the phase encode (cross stream) direction. The scan timing parameters were $\text{TE}=2.0 \text{ ms}$, $\text{TR}=4.9 \text{ ms}$, $\text{Venc}=225 \text{ cm/s}$ in the streamwise direction and 75 cm/s in the cross stream and spanwise directions. One 3D scan was completed in 2 min. 40 secs. The flow domain was scanned 12 times, and the data were averaged. The entire mean velocity experiment comprising 800,000 points was completed in less than one hour.

Backward Facing Step Steady Flow Loop

Both the MRV and PIV experiments used the same steady flow loop and test section. A centrifugal pump (Little Giant model no. TE-6MD-HC) circulated water at a flow rate of 77 L/min. In the MRV experiments, gadolinium-based contrast agent (Omniscan, Nycomed, Inc.) was added to the water in a concentration of 0.5%. The average volume flow rate was measured using a paddle wheel flow meter with an estimated uncertainty of 5%. The pump was placed approximately 3 meters from the magnet, and no other metallic parts were used in the loop.

Approximately 3 m of 2.54 cm ID flexible tubing was used between the pump and square channel test section. A barbed adapter is used between the tubing and a 5.1 cm diameter entrance to the test section. The test section is a square channel 5.1 cm by 5.1 cm by 65 cm. It has a development section 28 cm long with two 33% open area grids placed approximately 10 and 20 cm from the entrance. Figure 1a shows a photo of the downstream section with a

backward facing step created by a quarter of an acrylic tube with an outer radius of 3.2 cm. The MRI and PIV compatible test channel is made of clear acrylic. The test section exit which is 10 step heights downstream of separation is a 2.54 cm diameter hole. A barbed connector is used to connect 6 m of 2.54 cm ID flexible tubing which runs out the back side of the magnet bore and is connected to a large water reservoir.

PIV System

Calibration and comparison data were acquired on the flow centerplane using a conventional 2D DPIV system. The flow field was illuminated with two Continuum Minilite Nd:YAG lasers with 15 mJ/pulse at 532 nm and 10 Hz repetition rate. The beams from the lasers were combined using a Newport high-energy 532 nm polarizing beam splitter cube and a half wave retarder. Beam expanding optics were used to enlarge the diameter of the laser beam, and a spherical achromat lens with a 300 mm focal length and a cylindrical lens with a 125 mm negative focal length were used to produce a light sheet approximately $400 \mu\text{m}$ thick and 57 mm wide at the waist.

Images of flow tracers were captured with a Kodak ES1.0 8-bit digital camera. This interline frame transfer CCD camera has a 1018 by 1008 pixel array with a 60% fill factor and a pixel size of $9 \mu\text{m}$. A Micro-Nikkor lens (50 mm, 55 mm and 85 mm) was used in combination with extension rings to achieve a FOV 5.6 cm by 5.6 cm which covered the entire height of the channel and 1.75 step heights in the streamwise direction. Measurements were taken at three locations with the FOV centered at 1.3, 3, and 4.7 step heights downstream of the step.

The PIV image pairs were processed using the iterative 2D cross-correlation method developed by Westerweel (1997). The actual processing used a modified version of the code written by Han (2001). Each interrogation region (IR) consisted of 32×32 pixels thus giving a spatial resolution of 1.8 mm. With 50% overlapping IRs, a 62×62 velocity vector grid with a spacing of 0.9 mm was produced for each set of images. At each measurement location, 192 image pairs were used to calculate the turbulent flow statistics.

The accuracy of single-point PIV depends on the ability of tracer particles to follow the flow. Hollow spherical glass particles with 9 to 13 μm diameter and specific gravity of 1.1 (Potter Industries Inc.) were used. Uncertainty in magnification is estimated to produce uncertainty of 0.1% of the local flow velocity, while uncertainties related to calibration of the PIV system (calibration grid with respect to light sheet, angle of light sheet relative to flow direction, grid and camera) is estimated to ± 0.5 pixels. Processing 192 image pairs gave an uncertainty estimate of less than 1% for the local mean velocities and less than 8% for the local standard deviations.

RESULTS

All of the results presented are for flow with a Reynolds number equal to 48,000 based on the step height H and the freestream velocity at the step edge. Figure 1b shows a contour plot of the mean velocity magnitude measured in the centerplane using MRV. Velocities are

normalized by the mean bulk velocity at the edge of the step, U_{step} . The agreement between the MRV and PIV is excellent across the entire cross section of the channel and within the typical uncertainties for these measurements: +/- 5% in the repeatability of the flow rates between the PIV and MRV experiments and +/- 10% uncertainty in the MRV velocity measurements (Elkins et al. 2004).

Figure 2 illustrates the concept behind the turbulent velocity measurement technique. Four images from the centerplane of the flow are shown from scans with the bipolar gradient applied in the streamwise direction. The gradient amplitude is increased for the images a) to d). As the gradient strength increases, the regions of the flow with the largest turbulent velocity fluctuations become darker indicating lower signal strength due to the turbulent dephasing of the signal. This is most obvious in the separated shear layer since it contains the largest turbulent velocity fluctuations.

The rate of signal decay with increasing G^2 is found from a least squares fit of $\ln(S_0/S)$ vs. G^2 for each measurement voxel using data from the images with $G = 0, 2.5, 3.75,$ and 5 G/cm. The velocity variance at each point is found using the slope $[\ln(S_0/S)/G^2]$ in the equation $\sigma_u^2 = [\ln(S_0/S)/G^2]/h(\tau)$. Because $h(\tau)$ is related to the gradient sequence timing, it can be calibrated using one point from one component of the PIV measurements. Using the value $\sigma_u/U_{step} = 0.27$ at $x/H = 4.4, y/H = 0.7$ in the centerplane, $h(\tau) = 0.32$ (sec/G)². The velocity fluctuations throughout the entire 3D volume can be calculated once this constant is determined.

Figures 3a and 3b show contour plots of MRV and PIV values for σ_u/U_{step} and σ_v/U_{step} , respectively, in the centerplane of the flow. Here, σ_v is the standard deviation of the velocity fluctuations in the cross stream, y , direction. The MRV data are smoothed in these plots by averaging each data point with the values of its 6 neighboring points in the 3D domain. There is good agreement between the contour levels and patterns for the MRV and PIV for both σ_u/U_{step} and σ_v/U_{step} .

In order to better quantitatively compare the MRV and PIV measurements, plots of the cross stream profiles for σ_u/U_{step} and σ_v/U_{step} are shown in Figure 4 for the downstream position of $x/H = 4.4$. Error bars indicate the estimated uncertainty in the measurements. The calibration position is $x/H = 4.4$, so we expect MRV and PIV values to match here. The minimum uncertainty in the MRV curves is approximately 20% which is an estimate for the best performance one can expect from this method.

Both the MRV and PIV curves capture the displacement of the peak in the σ_u/U_{step} and σ_v/U_{step} profiles from $y/H = 1$, the height at which the shear layer originates. Both MRV and PIV curves agree in the recirculation and shear layer regions for $y/H < 1.1$.

However, the values in what remains of the freestream, $y/H = 1.1-1.5$, are underpredicted by the MRV, and some values are actually zero. This is related to the weak turbulence in this region. Here the decrease in signal due to turbulent dephasing is small and similar to the ghosting signal level combined with noise making it difficult to measure a change in signal with gradient amplitude.

DISCUSSION

The present technique provides a way to visualize turbulent flows (as seen in Figure 2d), and if applied correctly, it can provide accurate measurements of turbulent velocity variances. In order to achieve the best accuracy, one must consider several factors: characteristics of the turbulence including turbulent time scales and diffusion lengths, sequence parameters including gradient amplitude and timing (TE), and measurement volume and resolution.

Many previous derivations of this method have shown that the formula for predicting turbulent velocity fluctuations from signal loss due to turbulent dephasing is highly dependent on assumptions about the measurement time, TE , relative to the integral turbulent time scale, T_I . In our derivation, we make the assumption that TE is sufficiently short so that $R_L \approx 1$, i.e., much less than T_I . Kueth and Gao (1995) conclude that this is a good assumption when $TE < 0.1 * T_I$. In the backward facing step flow, an average T_I can be estimated to be 45 ms using $H/(U_{step}/2)$. Of course, the integral time scale varies as the shear layer develops, and a method such as that described by Gatenby and Gore (1994) could be used to measure both σ_u/U_{step} and T_I distributions. However, since $TE = 3.7$ ms was used for the measurements, the condition $TE < 0.1 * T_I$ holds in the entire flow domain except perhaps in the shear layer close to the step. This helps explain the close agreement with the PIV results except in the developing shear layer where estimates of T_I are less than 10 ms. In the developing shear layer at $x/H = 1$, the MRV and PIV measurements agree to within the uncertainty estimates except in the center of the shear layer.

Another important assumption made in this and other derivations is that the turbulent diffusion coefficient is locally constant around the measurement location. This assumption is justifiable if the spatial gradients of D_t are small. A relevant parameter to consider is the ratio between a length scale characterizing the variation of D_t and a diffusion length scale dependent on the measurement time. When this ratio is large, the turbulent dephasing of the magnetization signal comes from local diffusion related to the local value of the velocity variance. An appropriate length scale for the variation of D_t is the separated shear layer thickness. The measurement diffusion length scale can be estimated as $TE \cdot \sigma_u$. Considering a typical point in the separated shear layer, the shear layer thickness is around 1 cm, and the measurement diffusion length scale is less than

0.1 cm. The ratio of these two length scales is large, so our derivation should be valid throughout most of the flow except in the thin developing shear layer where the ratio can approach values close to 1. This, too, helps explain the disagreement between the PIV and MRV results seen in the developing shear layer in the contour plots in Figure 3 for $x/H < 2$.

Using lessons learned from this experiment, some guidelines can be presented that will help produce successful measurements in other flows. An appropriate spatial resolution should be chosen for the flow of interest. The SNR depends on the cube of the nominal voxel dimension, so a small compromise on image resolution can buy a large improvement in SNR. The flow experiment should be designed and the echo time (TE) chosen to satisfy the criterion $TE < 0.1 * T_1$. Next, preliminary scans should be performed to assess the loss of signal strength as a function of the bipolar gradient strength. Based on these results, G or M_1 should be chosen to produce signal losses ranging from 20-70%. If measurements will be done using only two scans, the nonzero value for G or M_1 should be chosen to produce a 50% maximum signal loss. A large number of signal acquisitions should be averaged to reduce statistical uncertainty and produce smooth results. Typically, the NSA should be >25 . Even with a large number of repetitions, the total scan time for the current test section was less than 12 minutes. An important implementation in our scanning sequence is that a complete set of 3D data in k-space was finished before the next acquisition was begun. This produces better averages of the large scale structures in the turbulence. The function $h(\tau)$ should be calibrated using a high value for the velocity fluctuation because smaller values for σ_u have higher uncertainty.

CONCLUSIONS

We have presented a method by which the turbulent velocity fluctuations can be measured in the entire flow field in a complex 3D geometry using MRI techniques. The method can be used to measure all three components of the fluctuating velocity. Results are presented for the streamwise and cross stream velocities in a backward facing step flow in a square channel. The results compare well with PIV measurements in the same flow. This method complements our previous MRV method for measuring the mean velocity field and allows us to measure the entire turbulent velocity field in complex geometries in and around potentially opaque objects using water or other MR compatible liquids and, in some cases, gases.

ACKNOWLEDGEMENTS

Christopher Elkins and John Eaton were supported by a grant from General Electric Aircraft Engines as part of the GE-University Strategic Alliance and a grant from the National Science Foundation (NSF CTS-0432478). Marcus Alley was supported by the same NSF grant and a grant from the National Institutes of Health (P41 RR09784).

REFERENCES

- Batchelor G. K., 1949: Diffusion in a field of homogeneous turbulence, Eulerian analysis. *Aust. J. Sci. Res.* 2, 437-450.
- De Gennes, P. G. (1969). Theory of spin echoes in a turbulent field. *Physics Letters A* 29(1): 20-21.
- Dyverfeldt, P., A. Sigfridsson, J. P. Kvitting and T. Ebbers (2006). Quantification of intravoxel velocity standard deviation and turbulence intensity by generalizing phase-contrast MRI. *Magn Reson Med* 56(4): 850-8.
- Elkins, C.J. et al (2004) Full-Field Velocity and Temperature Measurements Using Magnetic Resonance Imaging in Turbulent Complex Internal Flows. *International Journal of Heat and Fluid Flow* v.25, pp.702-710
- Elkins, C.J. et al (2003) 4D Magnetic Resonance Velocimetry for Mean Velocity Measurements in Complex Turbulent Flows. *Experiments in Fluids* v.34, pp. 494-503
- Gao, J. H. and J. O. Gore (1991). Turbulent flow effects on NMR imaging: Measurement of turbulent intensity. *Med Phys* 18(5): 1045-51.
- Gatenby, J. C. and J. C. Gore (1994). Mapping of turbulent intensity by magnetic resonance imaging. *J Magn Reson B* 104(2): 119-26.
- Gatenby, J. C., Gore, J.C. (1996). Echo-planar-imaging studies of turbulent flow. *J Magn Reson A* 121: 193-200.
- Han, D. (2001). Study of turbulent nonpremixed jet flames using simultaneous measurements of velocity and ch distribution, Stanford University.
- Kueth and Gao (1995). NMR signal loss from turbulence: Models of time dependence compared with data. *Physical Review. E, Statistical physics, plasmas, fluids, and related interdisciplinary topics* 51(4): 3252-3262.
- Kueth, D. O. (1989). Measuring distributions of diffusivity in turbulent fluids with magnetic-resonance imaging. *Physical Review. A* 40(8): 4542-4551.
- Li, T.Q et al. (1994). Turbulent pipe-flow studied by time-averaged NMR imaging - measurements of velocity profile and turbulent intensity. *Magnetic resonance Imaging* 12(6): 923-934.
- Westerweel, J. (1997). Fundamentals of digital particle image velocimetry. *Meas. Science & Tech.* 8(12): 1379-92.

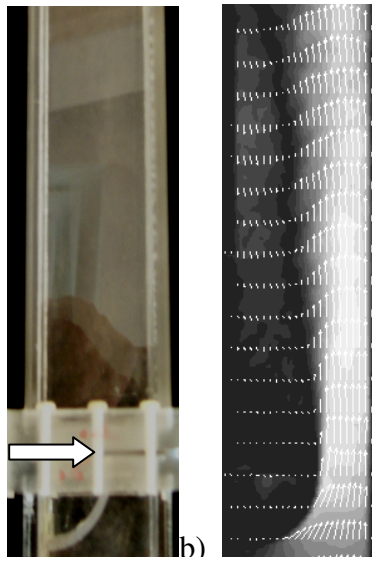


Figure 1: a) Photo of the test channel with a quarter round used to create a backward facing step (arrow indicates the position of the step), b) 2D cross section showing mean velocity magnitude contours and velocity vectors.

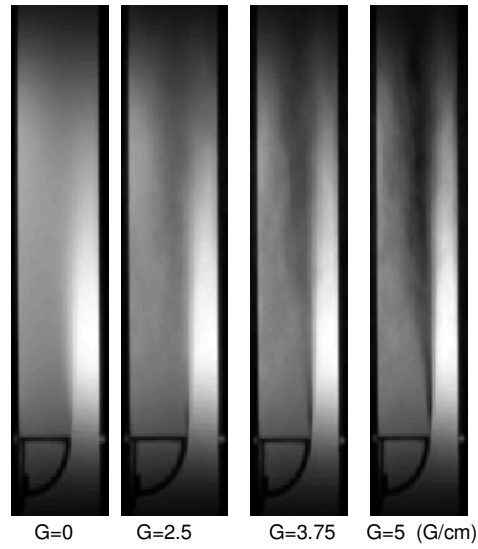


Figure 2: MR magnitude images of the centerplane of the flow acquired using increasing amplitudes for a bipolar magnetic field gradient applied in the vertical direction in order to measure the streamwise velocity fluctuation.

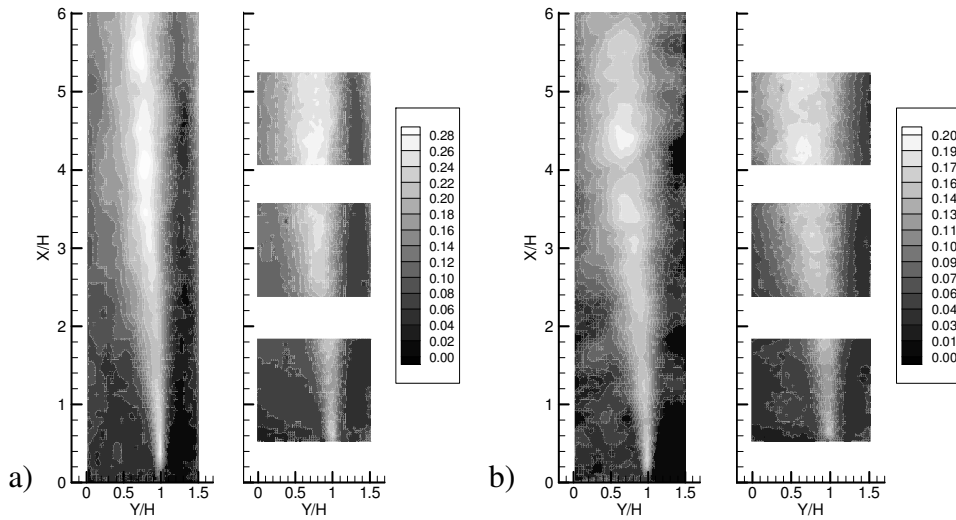


Figure 3: a) Contours of streamwise velocity fluctuation normalized by the freestream velocity at the step, σ_u / U_∞ measured with MRV (left) and PIV (right), b) contours of cross stream velocity fluctuation normalized by the freestream velocity at the step, σ_v / U_∞ measured with MRV (left) and PIV (right).

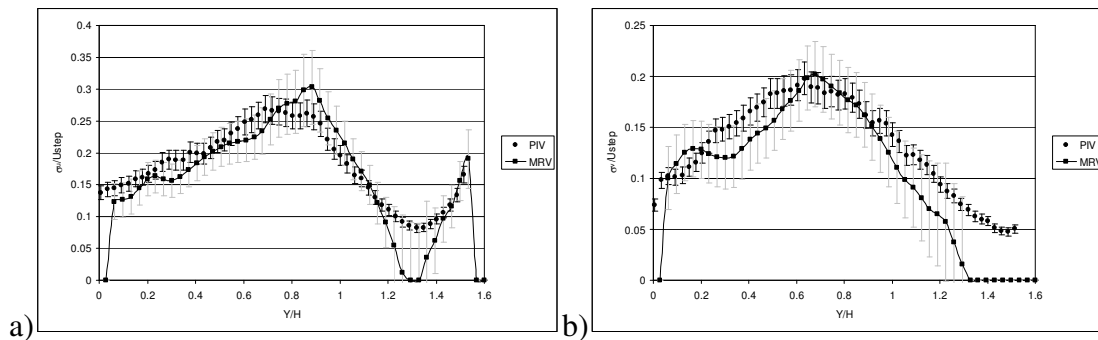


Figure 4: MRV and PIV cross stream profiles of σ_u / U_{step} and b) σ_v / U_{step} at $X / H = 4.4$, the calibration position. Error bars indicate estimated local uncertainty.